



Morphological Identification of Benthic Diatoms from Coral Reef Ecosystems of Bawean Island, East Jawa, Indonesia

Oktiyas Muzaky Luthfi*, Yenny Risjani, Rendha Agustina Ramawati, and Andrzej Witkowski

Received : September 9, 2025

Revised : December 22, 2025

Accepted : April 28, 2026

Online : May 31, 2026

Abstract

Small-sized benthic diatoms are frequently underrepresented in floristic surveys of coral reef ecosystems due to their inconspicuous morphology under light microscopy (LM). In this study, several benthic diatom strains were isolated into monoculture from coral reef substrates (sand, dead coral fragments, macroalgae, and surrounding seawater) collected at Bawean Island, East Jawa, Indonesia. The isolates were examined using LM and scanning electron microscopy (SEM) to clarify diagnostic morphological characters that are difficult to resolve with LM alone. Five taxa were documented: *Psammodictyon* sp., *Halamphora cf. oceanica*, *Halamphora yundangensis*, *Halamphora* sp., and *Nitzschia arauriae*. SEM observations revealed critical ultrastructural features, including raphe configuration, fibula structure, striae architecture, conopeum development, and internal valve morphology, which enabled more precise taxonomic evaluation and comparison with morphologically similar taxa. This work does not represent a comprehensive floristic inventory of reef-associated diatoms, but rather provides detailed SEM-guided morphological documentation of small (<20 µm), character-poor benthic taxa obtained in culture. These findings contribute taxonomic reference data for Indonesian marine diatoms and establish a morphological baseline for future integrative studies combining ultrastructural and molecular approaches.

Keywords: diatom taxonomy, *Halamphora*, morphological characters, *Psammodictyon*, reef-associated diatoms, scanning electron microscopy.

1. INTRODUCTION

Diatoms (*Bacillariophyceae*) represent one of the most diverse and ecologically important groups of microalgae in aquatic environments. They possess siliceous cell walls known as frustules, whose intricate morphology provides key characters for taxonomic identification [1]. Diatoms occur in a wide range of habitats, including planktonic environments, sediments, and various benthic substrates such as sand, rocks, macroalgae, and coral reef surfaces [2][3]. In coral reef ecosystems, benthic diatoms contribute significantly to primary productivity and form an important component of microbial communities associated with reef substrates [2][4].

Coral reef environments provide a complex mosaic of habitats that support diverse benthic diatom assemblages. These microorganisms

colonize substrates such as sand grains, coral rubble, dead coral skeletons, and macroalgal surfaces. Their ecological importance in reef systems has been increasingly recognized, particularly due to their role in primary production and their involvement in processes such as bioerosion of coral carbonate structures [3]. Despite their ecological significance, the taxonomy and diversity of benthic diatoms in coral reef habitats remain insufficiently documented in many tropical regions, including Indonesia.

Accurate taxonomic identification of diatoms relies primarily on detailed observations of frustule morphology. Light microscopy (LM) provides an initial assessment of valve shape, striae arrangement, and general valve architecture, whereas scanning electron microscopy (SEM) allows detailed examination of ultrastructural characters such as areolae morphology, raphe structure, and fine valve ornamentation [5][6]. SEM observations have proven particularly important for resolving taxonomic characters in several benthic diatom genera, including *Halamphora*, *Psammodictyon*, and *Tryblionella* [7]–[9].

Although coral reef habitats in Indonesia are known to harbor highly diverse diatom assemblages [2], detailed morphological documentation of many benthic taxa remains limited. The present study focuses on the morphological characterization of benthic diatoms collected from coral reef habitats of

Publisher's Note:

Pandawa Institute stays neutral with regard to jurisdictional claims in published maps and institutional affiliations.



Copyright:

© 2026 by the author(s).

Licensee Pandawa Institute, Metro, Indonesia. This article is an open access article distributed under the terms and conditions of the Creative Commons Attribution (CC BY) license (<https://creativecommons.org/licenses/by/4.0/>).

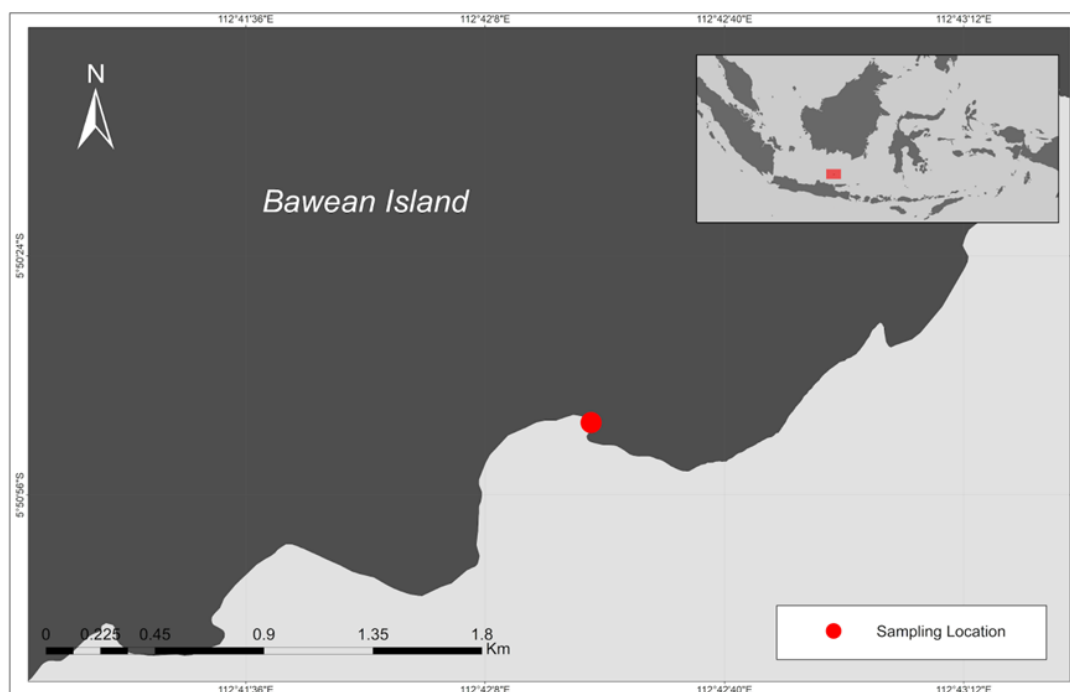


Figure 1. Sampling Location at Bawean Island.

Bawean Island, Indonesia. Using combined LM and SEM observations, this study aims to document the morphology and taxonomic identity of several benthic diatom taxa associated with reef substrates, thereby contributing additional taxonomic information for marine diatoms from Indonesian coral reef ecosystems.

2. MATERIALS AND METHODS

2.1. Materials

Guillard's F/2 medium (Merck KgaA), 10% hydrochloric acid (HCl), distilled water, and 30% hydrogen peroxide (H₂O₂, Sigma-Aldrich), Naphrax slides (Brunel Microscopes Ltd., Wiltshire, UK), polycarbonate membrane filter 2-20 μm (Nuclepore, Cytiva), gold-palladium (Ted Pella, Inc.), Zeiss Axio Imager M2 (Carl Zeiss, Oberkochen, Germany), and Hitachi SU8020 (Hitachi Ltd., Tokyo, Japan) were used in this work.

2.2. Methods

2.2.1. Sampling location

The research took place at the Hijau Daun Mangrove Ecotourism Area, on Bawean Island in Gresik Regency, East Java, Indonesia with coordinate 5°50'57.5"S, 112°43'3.6"E (Figure 1)

[3]. Bawean Island is located 120 km north of Java Island, within Gresik Regency, and its coastal areas have been recognized for their coral reef ecosystems, which support a variety of marine organisms as well as diverse benthic diatom habitats [10]. The selected study area provided optimal conditions because it contained diverse coral reef biodiversity alongside 3 key benthic diatom habitats, including sand, dead coral, and macroalgae [3]. The sampling period to observe diatom diversity was done within July–November 2023 because environmental conditions remained steady. Diatom sampling was conducted at approximately 10:00 a.m. (local time) to minimize potential photodamage from high solar irradiance and to preserve the viability and natural morphology of living diatom cells during transport to the laboratory [2].

2.2.2. Sampling Habitat and Collection

The research analyzed diatom samples obtained from the combination of sand, dead coral pieces, macroalgae, and sea water. The reef floor yielded samples that consisted of dead coral and sand which researchers collected by hand to minimize environmental disturbances. A proper anaerobic decomposition prevention method was achieved by filling 50 mL Falcon tubes in a 1:1:1 ratio of air,

seawater, and sample volume. To maintain sample integrity after collection, specimens were divided into 2 treatment groups. Non-preserved samples were stored in a cool, dark environment to ensure diatom viability for live observation. Meanwhile, preserved samples were treated with 90% ethanol to prevent microbial contamination and the degradation of diatom structures [11].

2.2.3. Diatom Isolation

Samples were then transferred to the Central Laboratory of Life Sciences at Brawijaya University, Indonesia and the Faculty of Chemical Technology and Laboratory of Diatom in University of Szczecin, Poland. Cell isolation used a Nikon Eclipse TS100 inverted microscope with 4×, 10×, and 40× magnification. Individual diatom cells were then transferred into plastic Petri dishes containing *f/2* medium [12] using modified Pasteur pipettes, ensuring the maintenance of monocultures [5]. This isolation process was repeated for many cycles until pure diatom cultures were obtained for growth in 100 mL Erlenmeyer flasks.

2.2.4. Sample Cleaning and Light Microscopy

Diatom frustules were cleaned following standard protocols with slight modifications [13]–[15]. Sediment samples were first treated with 10% HCl to remove carbonate components, and the reaction was allowed to proceed until effervescence ceased. The remaining residues were then oxidized with 37% H₂O₂ under gentle heating to eliminate organic matters. Oxidation was carefully monitored to avoid over-digestion of siliceous frustules, and the process was terminated once no visible organic material remained. After chemical treatment, the material was washed four times with distilled water, using cycles of decantation and centrifugation, until the supernatant reached a near-neutral pH. The cleaned suspensions were subsequently pipetted onto coverslips and mounted on glass slides with Naphrax®. Prepared slides were examined using a Zeiss Axio Imager M2 light microscope equipped with a 100× Plan Aplanachromat oil immersion objective (n.a. = 1.46) and differential interference contrast (DIC) optics. Photomicrographs were obtained with an AxioCam ERc5 digital camera (Carl Zeiss, Oberkochen, Germany).

2.2.5. SEM Investigation

For SEM observations, cleaned diatom suspensions were pipetted onto polycarbonate membrane filters with a pore size of 5 μm. After air-drying, the filters were mounted on 12.7 mm diameter aluminium pin stubs using conductive carbon adhesive. The specimens were then sputter-coated with a thin layer of gold–palladium to enhance conductivity and image quality. Observations were carried out using a SEM instrument at the West Pomeranian University of Technology and Rzeszów University.

2.2.6. Taxa Identification

Species identification was performed on cleaned diatom frustules using both LM and SEM. Taxonomic determinations followed established morphological criteria for diatom systematics [16], [17]. Diagnostic features assessed included valve symmetry, outline, length-to-width ratio, striae density and arrangement, areola structure, raphe morphology, and the configuration of central and terminal nodules. Particular attention was given to fine ultrastructural details observable under SEM, such as the nature of the areola occlusions, internal helictoglossae, and girdle band characteristics. Measurements of valve length, breadth, and striae density (number of striae in 10 μm) were also made.

3. RESULTS AND DISCUSSIONS

3.1. Overview of the Study Area

The northern East Java waters surrounding Bawean Island contain various coastal and marine ecosystems, including coral reefs with seagrass beds and mangrove forests [18]. The island provides an ecologically essential habitat for marine organisms through its combination of 19 coral reef patches spread throughout its waters. This region features vital ecosystem services because its reefs protect coasts and offer fishery resources together with biodiversity habitat [19]. Dead coral fragments along with sand and macroalgae formed potential surfaces for diatom attachment. Survey activities took place on coral reef patches with chosen structural complexity levels. The researcher studied 3 different reef habitats: the areas composed of sand, those covered by macroalgae and the coral

rubble locations. Sites maintained steady temperature conditions within 26–29°C and standard salinity measures from 33–35 PSU, but freshwater streams occasionally modified nearshore areas. Visual evaluation showed that diatoms existed extensively on macroalgal surfaces and sand pockets, as suggested in other studies of diatom community distributions [20].

3.2. Live Benthic Diatoms

From Figure 2, diatom taxa were classified into several life-habit categories: mobile, colonial, tube-forming, stalked, and pioneer. The tube-forming type represents a specific form of colonial organization, in which cells are embedded within mucilaginous tubes that provide protection while allowing limited movement. Pioneer taxa are characterized by their ability to rapidly colonize newly available substrates. This capacity is generally attributed to their small size, which reduces exposure to toxic compounds and minimizes assimilation of harmful substances [21]. The classifications applied here are based on established taxonomic and ecological references [21], [22].

The mucilage surrounding *Psammodictyon sp.* cell more closely resembles a diffuse mucilaginous

matrix or biofilm rather than a true tube (Figure 2 (a)) [23]. In contrast, *Halamphora oceanica* and *Halamphora sp.* were predominantly found in colonial forms, ranging from compact clusters to paired cells, suggesting a flexible growth strategy that enhances persistence under variable environmental conditions [24]. The presence of *Nitzschia arauraea* in colonies attached within biofilm structures highlights its ecological plasticity; although *Nitzschia* is typically classified as motile, its colonial occurrence indicates an alternative survival strategy under biofilm-dominated habitats [25][26]. The coexistence of these growth forms within the studied assemblages suggests a dynamic response to environmental conditions, where protective tube-forming species may indicate relatively good water quality, while colonial assemblages contribute to the structural complexity and resilience of biofilms [27].

3.3. Light and Scanning Electron Microscopy

3.3.1. *Psammodictyon sp.*

The valves of *Psammodictyon sp.* were panduriform with a distinctly constricted median portion, measuring 10.3–15.7 µm in length and 5.3 – 5.9 µm at the widest part (Figure 3(a)). External

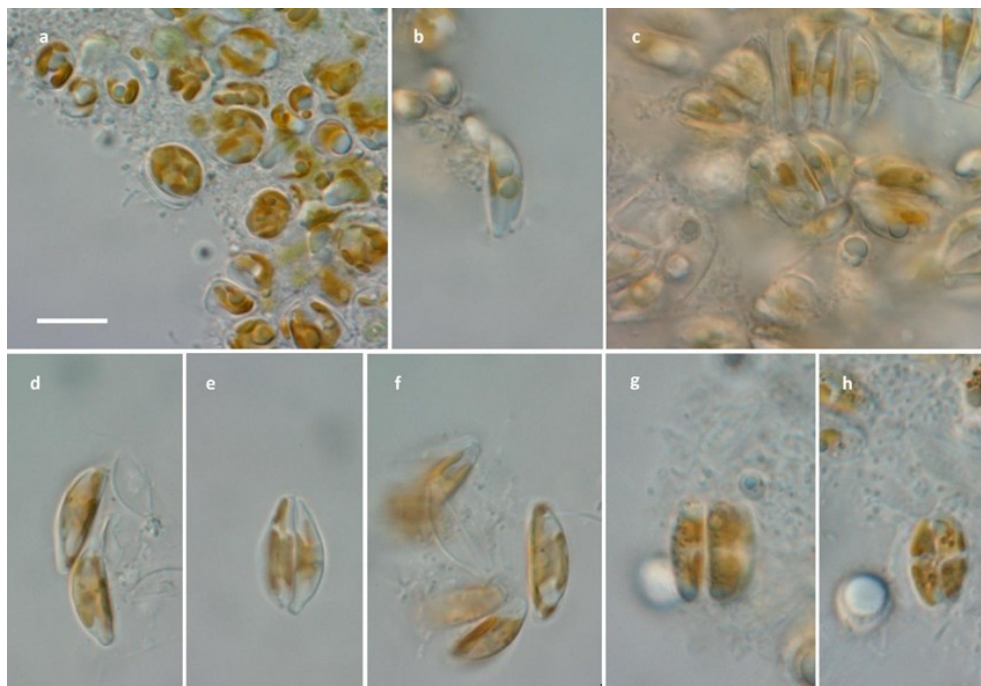


Figure 2. Live diatoms under 100× magnifications. (a) *Psammodictyon sp.* in tube formation; (b, c) colonial cells of *Halamphora oceanica*; (d, f) colony and some dead colony with light color and (e) two single cells of *Halamphora sp.*; (g, h) colony of *Nitzschia arauriae* that attached by biofilm. Scale bar a–h = 10 µm.

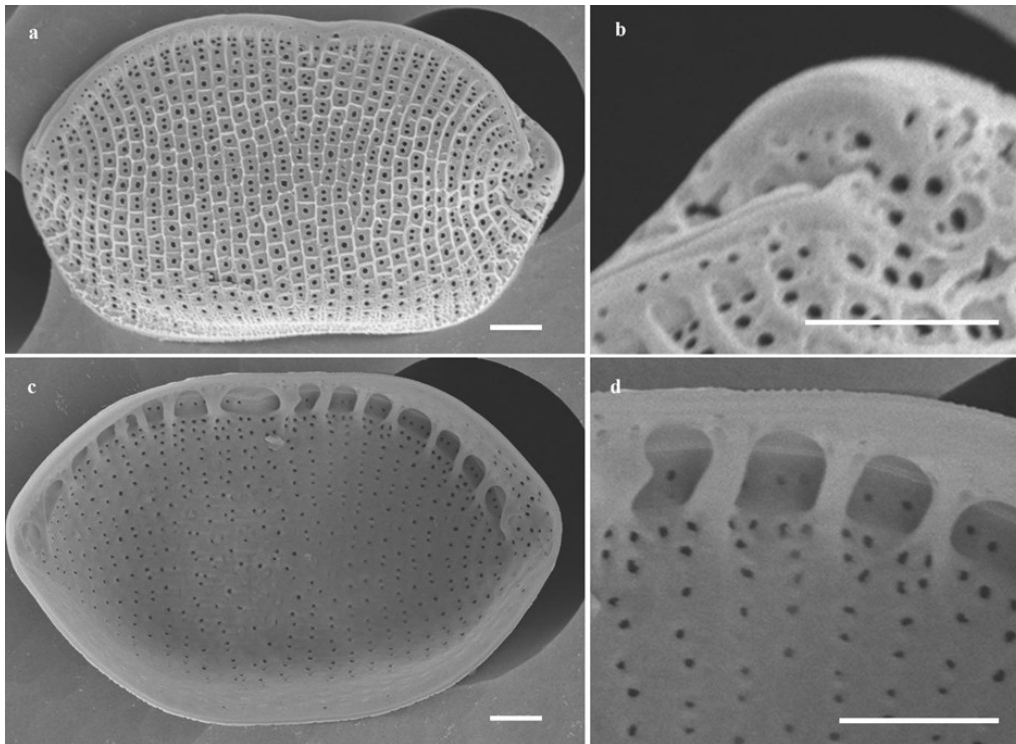


Figure 3. SEM results of *Psammodictyon* sp. reveal various ornamental structures: (a) The entire external view; (b) the external view of the diatom apex; (c) the entire internal view; (d) the keeled eccentric raphe, and fibulae. Scale bars a–d = 1 μ m.

and internal views of the valve were shown in Figures 3(a) and 3(b). The valve surface was slightly convex, exhibiting an undulate outline as illustrated in Figure 3(a). Figure 3(c) displayed the apex of the diatom, while the internal keel was clearly visible in Figure 3(d). The keel and raphe were positioned eccentrically along the margin and supported by 14 fibulae, spaced at approximately 10 μ m intervals. The striae were uniseriate, numbering 27–31 per 10 μ m, and were distinctly visible in the external view. The panduriform to broadly linear valve shape, with narrowing at the central margin, was comparable to the morphology described for *Tryblionella* [9][28][29]. SEM observations further confirmed the presence of the eccentric raphe and fibulae in the internal view.

Taxonomically, members of the genera *Psammodictyon* and *Tryblionella* had previously been placed within *Nitzschia* due to their morphological similarities, such as raphe symmetry within the frustule, and the presence of an eccentric raphe (Table 1). The raphe symmetry refers to the diagonally opposed arrangement of the raphe branches on the valves, which is a defining characteristic of the *Nitzschiaceae*. Subsequent

ultrastructural investigations have demonstrated that generic delimitation among these taxa cannot rely solely on valve outline or degree of constriction. In accordance with recent taxonomic revisions [9], *Psammodictyon* is distinguished by a relatively simple marginal keel with discrete fibulae and the absence of a pronounced marginal ridge or strong longitudinal valve undulation. In contrast, *Tryblionella sensu stricto* is characterized by combinations of features including a distinctly undulate valve face, development of a marginal ridge, and squat or solid fibulae associated with a more complex raphe canal architecture [28][30].

The specimens illustrated in Figure 3 show superficial similarity to several panduriform taxa, including *Tryblionella persuadens* Chohn. and *Psammodictyon rudum* [31]–[34], particularly in overall valve outline. *Tryblionella persuadens* differs from the present material in having higher striae densities (ca. 32 in 10 μ m) and in lacking the typical loculate areolae and panduriform valve architecture characteristic of *Psammodictyon*. In comparison with *P. rudum*, partial overlap exists in valve size, but that species generally exhibits larger valves and slightly lower striae densities (28–30 in

Table 1. Morphological comparison between the Bawean specimens and morphologically similar taxa.

Characters	<i>Psammodictyon</i> sp. (This study)	<i>T. persuadens</i> [32]	<i>P. cf. constrictum</i> [33]	<i>P. constrictum</i> [34]	<i>P. rudum</i> [35]
Valve outline	Panduriform	Linear-elliptic	Panduriform	Panduriform	Panduriform-linear
Median constriction	Weak-moderate	Absent	Distinct	Slight	Slight
Valve length (μm)	10.3–15.7	~16–20	17.3–18.0	~20–21	12–20
Valve width (μm)	5.3–5.9	~6	7.6–8.6	7.0–7.5	5.5–6.5
Striae in 10 μm	27–31	~32	~23	15–18	28–30
Fibulae in 10 μm	~14	fewer	~16	poorly defined	10–14
Areola structure	loculate polygonal	fine	rounded-polygonal	hexagonal loculate	coarse irregular
Raphe	eccentric marginal	eccentric	eccentric	eccentric	eccentric
Raphe termination	distal end not reaching apex	reaching apex	reaching apex	reaching apex	reaching apex
Striae pattern	slightly irregular	regular	regular	regular	regular

10 μm) as well as fewer fibulae.

A closer comparison can be made with the small-celled taxa recently reported from coastal waters of Viet Nam, reported previously [33], which were identified as *Psammodictyon cf. constrictum*. These Vietnamese specimens also exhibit panduriform valves belonging to the *P. constrictum* complex, but they are consistently larger (17.3–18 μm long and 7.6–8.6 μm wide) and possess lower striae densities (ca. 23 in 10 μm) than those observed in the Bawean material. Furthermore, the Bawean specimens show slightly irregular striation patterns in the dorsal central region, including local convergence of adjacent striae. In addition, the distal raphe end on the right side of the valve does not reach the valve apex, giving the raphe a slightly curved appearance.

SEM observations also reveal a decussate arrangement of loculate areolae forming irregular transapical striae, a structural feature consistent with the valve architecture typically reported for *Psammodictyon*. Taken together, the Bawean specimens share the general panduriform valve morphology and internal valve architecture characteristic of the genus but differ from both the classical concept of *P. constrictum* and other similar taxa such as *P. rudum* and *Tryblionella persuadens* in valve size, striae density, and raphe termination. Because none of the currently described taxa correspond precisely to the combination of characters observed here, the Bawean material is conservatively treated as *Psammodictyon* sp.

3.3.2. *Halamphora cf. oceanica*

SEM observations revealed the valve morphology of *Halamphora cf. oceanica*, as illustrated in Figure 4. Based on observations of multiple valves under LM and SEM, valve length ranges from 11.2–16.6 μm in length and 3.1–4.3 μm in width. The dorsal margin was broader than the ventral margin. A straight raphe extended along the ventral side, reaching a length of 6.9 μm (Figure 4(a)). The apices were rostrate, i.e. beak-like or rounded at the ends of the valve (Figures 4(a)–4(b)). The striae were biseriate, numbering 18–23 in 10 μm , with distinct areolae clearly visible (Figure 4(b)).

To clarify the taxonomic placement of the Bawean population, the specimens identified here

as *Halamphora cf. oceanica* were compared with several morphologically similar taxa within the genus *Halamphora*. In addition to *H. oceanica*, the comparison includes *H. nipponensis*, *H. subacutiuscula*, *H. pertusa*, and *H. yundangensis*, which exhibit comparable valve outlines or overlapping size ranges. Diagnostic characters such as valve dimensions, striae density, striae structure, apex morphology, and raphe configuration were examined. The principal morphological differences between the Bawean specimens and these taxa are summarized in Table 2.

SEM analysis revealed that the external raphe

endings curved slightly toward the dorsal margin, while the internal helictoglossae were weakly developed. The dorsal striae are uniseriate, with the areolae externally occluded by cribra (Figure 4(a)). These occlusions were previously misinterpreted as a biseriate arrangement and have now been corrected. A distinct conopeum, attached to the raphe system, interrupts the dorsal striae near the dorsal margin [39]. The Bawean specimens identified as *Halamphora cf. oceanica* share several general morphological features with *H. oceanica*, including small valve dimensions and a dorsiventral semi-elliptical valve outline. However, clear

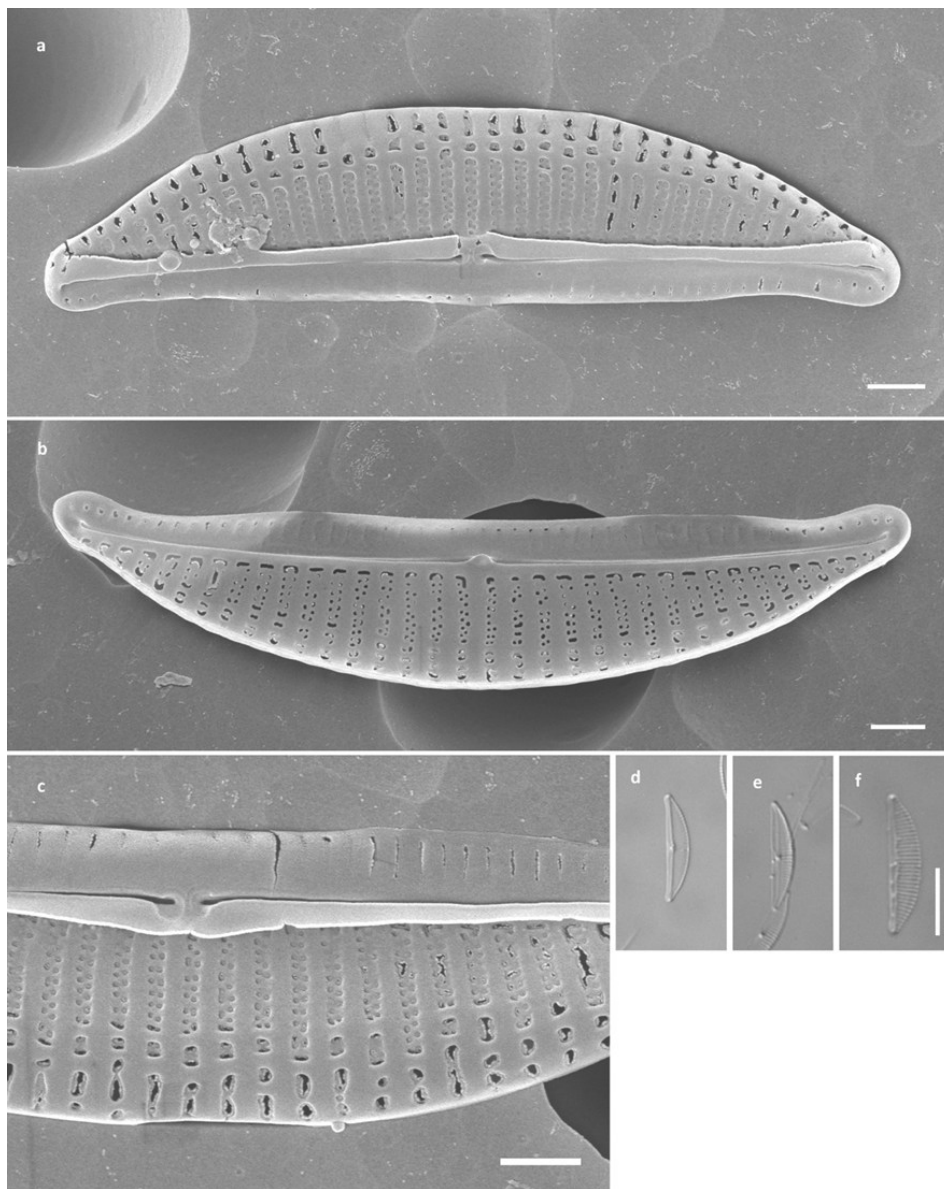


Figure 4. *Halamphora cf. oceanica* from Bawean Island observed under SEM and LM. (a) External valve view; (b) internal valve view; (c) detail of the central valve area showing simple proximal raphe endings; (d–f) LM images of valves in dorsal view with clearly visible dorsal striae. Scale bars: a–c = 1 μm ; d–f = 10 μm .

Table 2. Diagnostic morphological characters distinguishing the Bawean *Halamphora* taxa (*Halamphora cf. oceanica* and *Halamphora* sp.) from morphologically similar species of *Halamphora* based on published descriptions.

Species	Valve outline	Length (µm)	Width (µm)	Dorsal striae (10 µm)	Striae structure	Apex shape	Diagnostic characters	Reference
<i>Halamphora cf. oceanica</i> (Bawean Island)	Semi-elliptical, dorsiventral	11.2–16.6	3.1–4.3	18–23	Biseriate	Rostrate	Small valves; dorsal margin broader than ventral margin; distinct areolae	This study
<i>Halamphora</i> sp. (Bawean Island)	Semi-elliptical, dorsiventral	15.7–17.8	3.3–3.8	21–25	Biseriate	Rostrate	Straight ventral raphe (~8.7 µm); 12–15 areolae per stria	This study
<i>Halamphora oceanica</i>	Semi-elliptical	9–17	2.5–5.0	28–34	Biseriate	Rounded	Hyaline longitudinal band along dorsal margin	[36]
<i>Halamphora nipponensis</i>	Narrowly semi-elliptical	18–29	3.5–4.0	21–23	Areolate	Rounded	Distinct ventral fascia	[37]
<i>Halamphora subacutiuscula</i>	Semi-elliptical to semi-lanceolate	13–34	3.5–5.5	18–22	Areolate	Protracted	Dense ventral striae	[37]
<i>Halamphora pertusa</i>	Elliptic-lanceolate	17–34	4–6	17–19	Areolate	Subcapitate	Longitudinal silica band near dorsal axial area	[38]
<i>Halamphora yundangensis</i>	Semi-lanceolate	13.0–39.5	3.5–5.5	17–21	Biseriate internally	Capitate / rostrate	Prominent dorsal marginal ridge forming hyaline band	[8]
<i>Halamphora halophila</i>	Semi-elliptical	29–33	4.5–5.0	21–22	Areolate	Weakly protracted	Distal raphe ends dorsally hooked	[37]
<i>Halamphora turgida</i> var. <i>lacustris</i>	Semi-elliptical	27–48	6–8	10–11	Biseriate	Subcapitate	Heavily silicified valves; dorsal striae interrupted by marginal ridge	[37]

differences are observed in the structure and density of the striae. In the Bawean material, the striae are uniseriate and number 18–23 in 10 μm , whereas *H. oceanica* typically possesses biseriata dorsal striae with a considerably higher density of 28–34 in 10 μm . Such differences in striae architecture represent an important diagnostic character within the genus *Halamphora* and suggest that the Bawean population does not fully correspond to the original description of *H. oceanica*.

Comparisons with other morphologically similar species further support this interpretation. *Halamphora nipponensis* differs in having narrowly semi-elliptical valves with more elongated proportions and rounded apices. *Halamphora subacutiuscula* is characterized by semi-lanceolate valves with distinctly protracted apices and much denser ventral striae. *Halamphora pertusa* can be distinguished by its elliptic-lanceolate valve outline and the presence of a longitudinal silica band near the dorsal axial area [37]. In contrast, *Halamphora yundangensis* possesses semi-lanceolate valves with capitate apices and a prominent dorsal marginal ridge forming a broad hyaline area. These

characters are not observed in the Bawean material.

Taken together, these comparisons indicate that although the Bawean specimens share certain general morphological similarities with several described species of *Halamphora*, none of the currently known taxa correspond precisely to the observed combination of characters. The Bawean population most closely resembles *H. oceanica* in overall valve size and general morphology, but differs in several diagnostic characters, particularly in striae structure and density. Consequently, the material is conservatively treated here as *Halamphora cf. oceanica* pending further studies, including molecular analyses, which may help clarify whether the Bawean population represents an undescribed species or a morphological variant of an existing taxon.

3.3.3. *Halamphora yundangensis*

The overall valve morphology of *Halamphora yundangensis* was revealed by SEM observations (Figure 5). As shown in Figures 5(e)–5(f), the species exhibited a dorsiventral outline, measuring 13.7–25.6 μm in length and 2.9–4.7 μm in width.

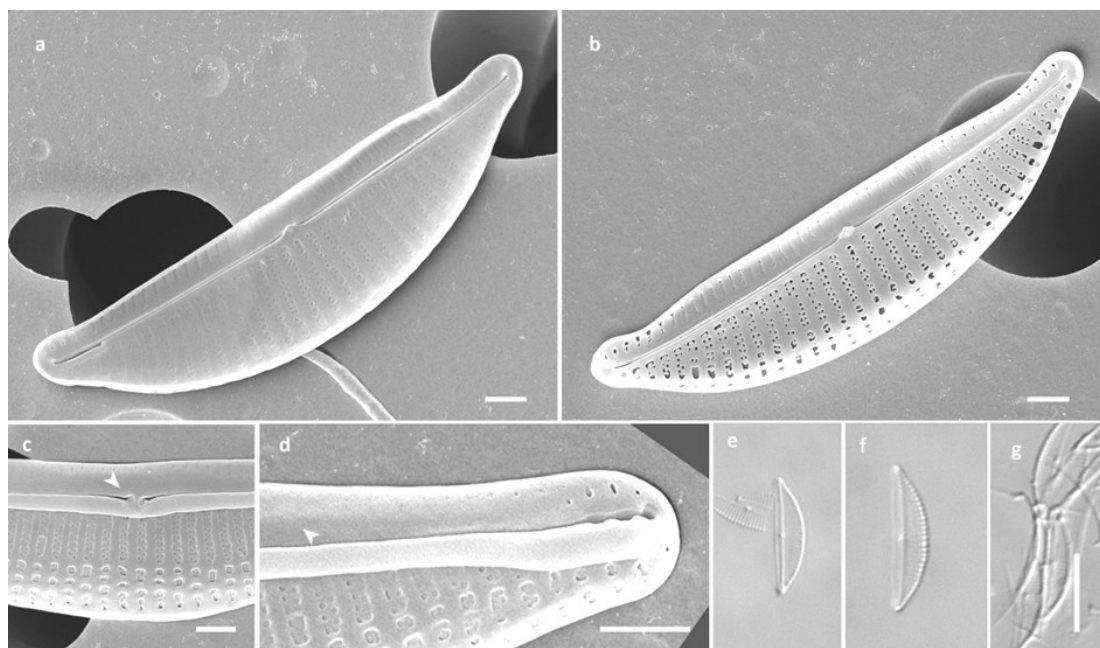


Figure 5. *Halamphora yundangensis* from Bawean Island observed under scanning electron microscopy (SEM) and light microscopy (LM). (a) Internal view of the valve; (b) Internal view of the central valve area, illustrating the raphe terminating at fused central helictoglossae; (c) external view of the valve central area, including the tear drop-shaped proximal raphe endings; (d) external view of valve apex, showing simple distal raphe ending; (e–g) LM. (e, f, h) valves on dorsal view with clear dorsal striae; (g) girdle bands. Scale bars: a–d = 1 μm , e–h = 10 μm .

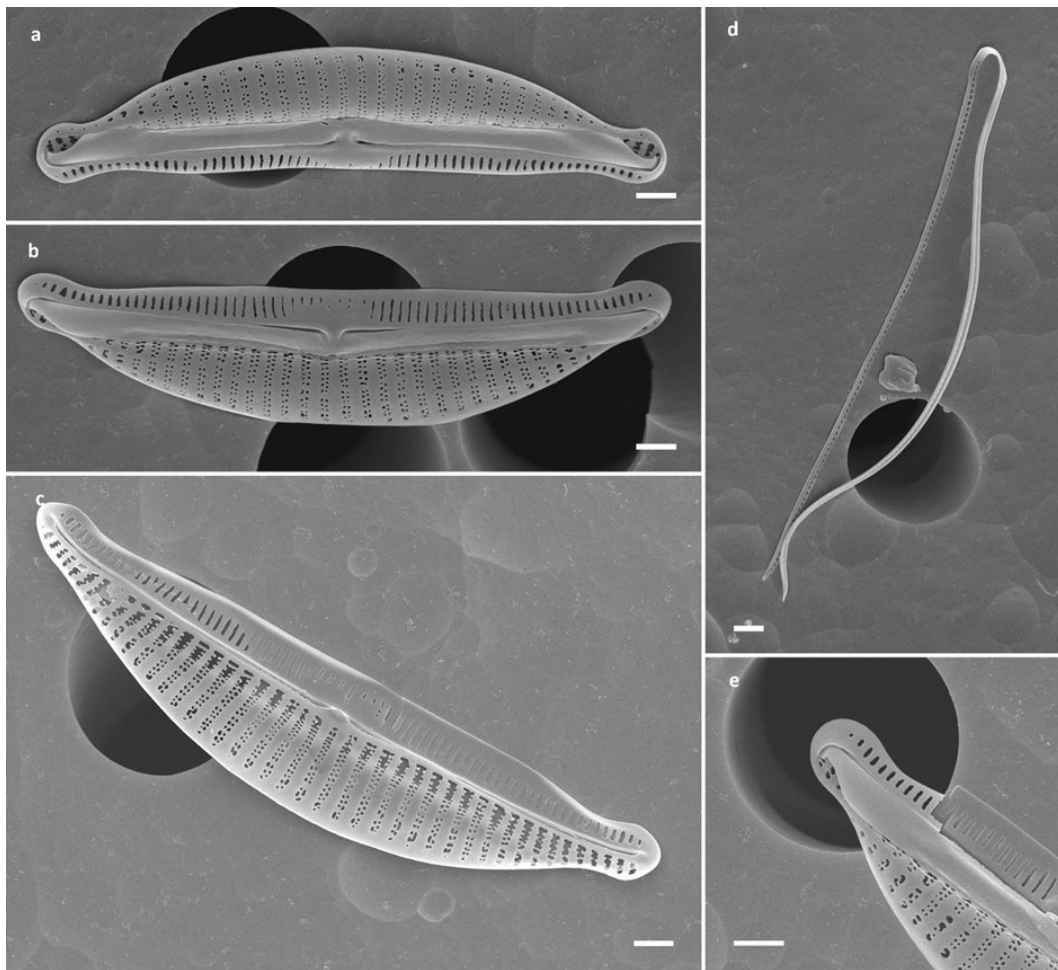


Figure 6. *Halamphora* sp. observed under scanning electron microscopy (SEM). (a, b) External view of valve; (c) internal view of valve; (d) girdle band; (e) external view of valve apex, showing distal raphe ending bending to dorsal side. Scale bars = 1 μm .

The dorsal margin was broader than the ventral margin. A straight raphe extended along the ventral side, reaching 8.3 μm in length (Figure 5(a)). The apices were rostrate, i.e. beak-like or rounded at the valve ends (Figure 5(d)). The striae were biseriate, arranged at a density of 19–20 in 10 μm (Figure 5 (c)).

Halamphora yundangensis displayed several diagnostic characters that distinguished it from related taxa. In the present material, *H. yundangensis* is characterized by a conspicuously broad dorsal margin forming an extensive hyaline area (arrow head Figures 5(c)–5(d)), external dorsal striae expressed as interrupted transapical slit-like structures, and internally biseriate striae that become shortened and reduced near the raphe. The dorsal striae internally were biseriate but merged into a uniseriate of areolae near the raphe, while the central area remained devoid of areolae. One to

three poroids were observed near the ventral apices, and the raphe endings formed distinct helictoglossae at the central nodule. This species could be confused with *H. foramina* due to their similar semi-lanceolate valve outline, rounded knob-like apices, and biseriate dorsal striae. However, *H. yundangensis* differed by possessing a wider dorsal margin, a more extensive hyaline area, and a higher striae density compared with *H. foramina* [5].

In addition to *Halamphora foramina*, another species showing partial morphological similarity to the present material is *Halamphora ghanensis* Levkov [40]. Both *H. yundangensis* and *H. ghanensis* share relatively small valve dimensions and internally biseriate dorsal striae that become uniseriate near the raphe. The valves of both species are distinctly dorsiventral, with a semi-elliptical outline, a strongly convex dorsal margin, and a comparatively straight ventral margin. However, *H.*

ghanensis differs from *H. yundangensis* in having a narrower dorsal margin, a less extensive central hyaline area, and a lower dorsal striae density (14–16 in 10 μm in *H. ghanensis* versus 17–21 in 10 μm in *H. yundangensis*). In addition, the valve width of *H. ghanensis* (5.0–5.6 μm) is generally greater than that observed in *H. yundangensis* (3.5–5.5 μm), and the external dorsal striae in *H. ghanensis* are more distinctly biseriate toward the dorsal margin. These consistent morphometric and structural differences support the separation of *H. yundangensis* from *H. ghanensis* despite their partial resemblance.

3.3.4. *Halamphora* sp.

The general valve morphology of *Halamphora* sp. was documented by SEM (Figure 6). As shown in Figures 6(a)–6(c), the species exhibited a dorsiventral outline, measuring 15.7–17.8 μm in length and 3.3–3.8 μm in width. The dorsal margin was broader than the ventral margin. A straight raphe extended along the ventral side, with a total length of 8.7 μm (Figure 6(a)). The apices were rostrate, i.e. beak-like or rounded at the ends of the valve (Figure 6(e)). The striae were biseriate, arranged at a density of 21–25 in 10 μm , with areolae clearly visible (Figure 6(c)). The average number of areolae in the central portion ranged from 12–15 per stria. The observed specimens exhibit the main diagnostic characters of the genus *Halamphora*, including dorsiventral valves with the raphe positioned along the ventral margin and supported by a marginal raphe ledge. This raphe configuration distinguishes *Halamphora* from species of the genus *Amphora*, in which the raphe is typically embedded within a broader raphe canal and the girdle structure shows a different organization of the girdle bands.

The Bawean specimens differ from *Halamphora* cf. *oceanica* in possessing biseriate striae (21–25 in 10 μm) and slightly larger valve proportions. They also differ from *Halamphora yundangensis* in lacking a prominent dorsal marginal ridge forming a broad hyaline band along the junction of the valve face and dorsal margin. In overall valve morphology, the Bawean specimens show a closer resemblance to *Halamphora turgida* var. *lacustris* [37]. However, the present material differs from that taxon in its considerably smaller valve dimensions (15.7–17.8 μm long and 3.3–3.8 μm

wide versus 27–48 μm long and 6–8 μm wide in *H. turgida* var. *lacustris*) and in the structure of the ventral striae. In the Bawean specimens the ventral striae are continuous across the valve center, whereas in *H. turgida* var. *lacustris* the ventral striae are interrupted at the valve center. The Bawean material also differs from larger taxa such as *Halamphora halophila* in its markedly smaller valve size. Because the available material is limited and the observed combination of characters does not correspond fully to any described species, the taxon is conservatively treated here as *Halamphora* sp.

3.3.5. *Nitzschia aurariae* Cholnoky

As shown in Figures 7(e)–7(h), *Nitzschia aurariae* exhibited a linear-elliptic valve outline, with valve length ranging from 7.7–12.1 μm and valve width from 2.6–3.7 μm . The valves possessed an eccentric raphe positioned along one margin and supported by regularly spaced fibulae, which were visible in both SEM and LM observations (Figure 7(b)). Due to the absence of internal valve views, no inference was made regarding the presence or absence of a central nodule. The striae were clearly visible, with a density of 24–28 in 10 μm and fibulae 7–12 in 10 μm (Figure 7(d)).

Members of the genus *Nitzschia* are generally characterized by fine striae, valves ranging from linear-lanceolate in larger specimens to elliptic in smaller ones, and apices that vary from acute to rounded [41]. The genus is also taxonomically challenging due to the wide morphological diversity of its members. Valve length ranges from very small species (e.g. 3–17 μm in *N. soratensis*) to extremely large taxa exceeding 300 μm and reaching up to 600 μm in some marine species (e.g. *Nitzschia ventricosa*), with valve width varying from a few micrometres to more than 15 μm . Striae density likewise spans a wide spectrum, from coarse striation visible in LM (e.g. 9–14 striae in 10 μm in *N. pungens*) to extremely fine striation requiring SEM resolution (exceeding 40 and up to 70–78 striae in 10 μm in species such as *N. dentatum*) [29][41]–[43]

SEM observations of *N. aurariae* in this study confirmed the linear-elliptic outline with broadly rounded apices and a keel system located along one valve margin. The eccentric raphe was clearly

visible in external valve view (Figure 7(c)), whereas fibulae were not resolved in this view and were observed only in LM images (Figures 7(e)–7(g)). The arrangement of areolae was not fully developed; in some parts, the areolae remained partially occluded by silica. The material of *N. arauriae* examined here appeared somewhat imperfect, likely due to attributed to culture-related artifacts rather than to overexposure during the cleaning procedure. In particular, growth under artificial culture conditions may have promoted the retention of extracellular organic material or biofilm residues on the valves, which can obscure fine ultrastructural details even after chemical treatment.

Nitzschia arauriae, *N. ovalis*, *N. inconspicua*, and *N. frustulum* share several general morphological features, including small linear-elliptic valves and an eccentric raphe supported by regularly spaced fibulae, resulting in a superficial similarity among these taxa in light microscopy observations [44][45]. Nevertheless, these species can be distinguished by differences in valve

dimensions, striae density, and fibula spacing. *Nitzschia arauriae* is characterized by comparatively small and delicate valves measuring 7.7–12.1 μm in length and 2.6–3.7 μm in width, with an elongated linear-elliptic to narrowly elliptic outline, 24–28 striae in 10 μm , and 7–12 fibulae in 10 μm . In contrast, *Nitzschia ovalis* possesses distinctly larger and wider valves (13–22.5 μm long and 4.5–4.6 μm wide) with a similar valve outline but is readily distinguished by a much higher striae density (approximately 42 striae in 10 μm) and more closely spaced fibulae (12–16 in 10 μm). *Nitzschia inconspicua* generally exhibits valves 6–30 μm long and 2–3 μm wide, typically narrower than those observed in the present material, with comparable striae densities and regularly spaced fibulae [44]. Although *Nitzschia frustulum* shows a similar general valve outline, it typically possesses consistently wider valves, commonly exceeding 3 μm in width, giving the species a more robust appearance [44]. Considering these morphometric differences collectively, the Bawean specimens fall

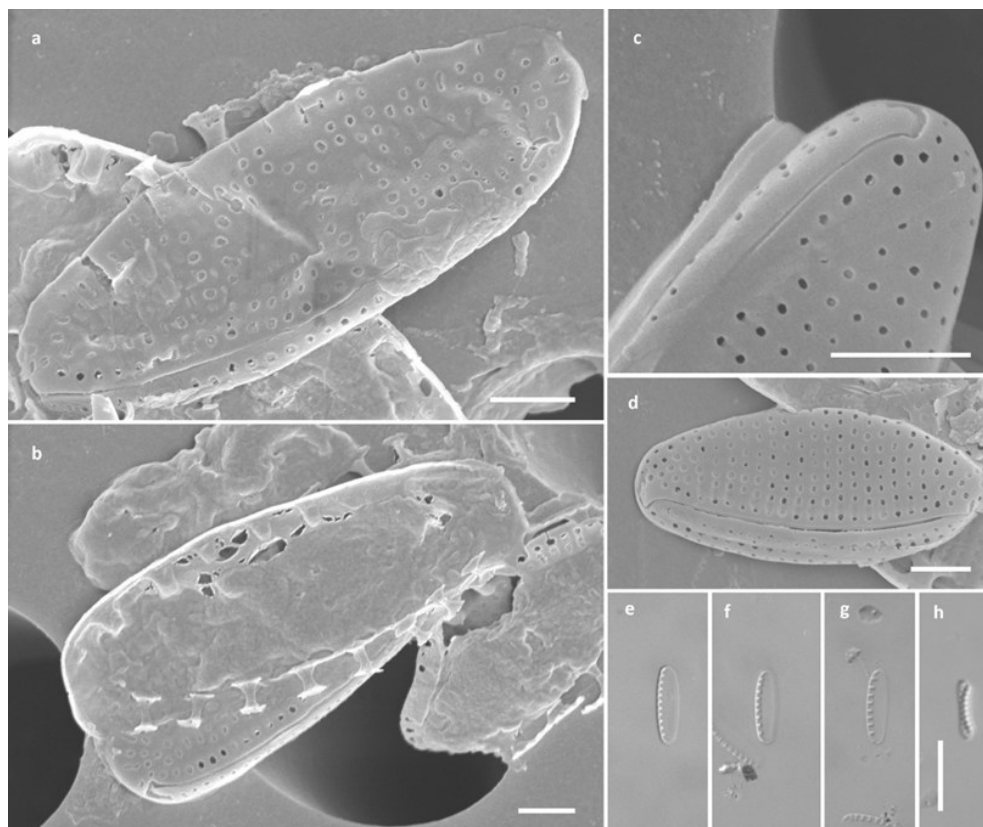


Figure 7. *Nitzschia arauriae* under scanning electron microscopy (SEM) and light microscopy (LM). (a) External view of valve (b) broken fibulae visible on top of a frustule; (c) hook-like distal raphe ends; (d) external view of valve, illustrating eccentric raphe; (e–h) LM. (e–g) valves with observed fibulae; (h) girdle view. Scale bars: a–d = 1 μm , e–h = 10 μm .

Table 3. Morphometric characteristics of the diatom taxa recorded in this study.

No	Morphometric character	<i>Psammodictyon</i> sp.	<i>Halamphora</i> cf. <i>oceanica</i>	<i>Halamphora yundangensis</i>	<i>Halamphora</i> sp.	<i>Nitzschia arauriae</i>
1	Length (μm)	10.3–15.7	11.2–16.6	13.7–25.6	15.7–17.8	7.7–12.1
2	Width (μm)	5.3–5.9	3.1–4.3	2.9–4.7	3.3–3.8	2.6–3.7
3	Striae (in 10 μm)	27–31	18–23	19–20	21–25	24–28
4	Raphe structure	marginal keel	ventral raphe	ventral raphe	ventral raphe	eccentric raphe
5	Raphe position	eccentric	ventral margin	ventral margin	ventral margin	eccentric
6	Cell pigmentation	slightly brownish-yellow	yellow	absent	slightly brownish-yellow	slightly brownish-yellow

Note: "absent" indicates that pigmentation was not observed

within the dimensional range reported for *Nitzschia arauriae* and are therefore consistent with the morphology of this species. Morphometric ranges of the Bawean specimens and comparable taxa are summarized in Table 3.

The biometric data used in this study include length, width, and striae density, while the morphological data include raphe, raphe position, and diatom pigment color. The length of the diatoms found varies depending on the species. The longest species recorded was *Halamphora* sp., with a length of 17.8 μm , whereas the shortest species recorded was *Psammodictyon* sp., with a length of 15.7 μm (see Table 3). The species with the greatest width was *Psammodictyon* sp. (5.9 μm), while the species with the smallest width was *Halamphora* cf. *oceanica* (4.3 μm). The highest number of striae per 10 μm was found in *Psammodictyon* sp., ranging between 27–31 striae, while the lowest number of striae was found in *Halamphora yundangensis*, with 19–20 striae, as listed in Table 3. Raphe was found in *Psammodictyon* sp. In *Halamphora* cf. *oceanica*, *Halamphora yundangensis*, and *Halamphora* sp., a straight elongated raphe was observed, located on the ventral margin or the central part of the body. In *Nitzschia arauriae*, the raphe was found on the edge. A yellow pigment color was observed in *Halamphora* cf. *oceanica*, while a slightly brownish-yellow pigment color was observed in three species studied: *Psammodictyon* sp., *Halamphora* sp., and *Nitzschia arauriae*.

3.4. Taxonomic Remarks

Studies of coral reef habitats have demonstrated that benthic diatom assemblages associated with reef substrates can be highly diverse, often comprising numerous taxa inhabiting coral fragments, sediments, and macrophyte surfaces. However, the present study focuses on the morphological characterization of several cultured benthic diatoms obtained from coral reef environments of Bawean Island rather than on documenting the full floristic diversity of the reef-associated assemblage. The taxa documented here belong to genera commonly reported from marine benthic environments, including *Psammodictyon*, *Halamphora*, and *Nitzschia*. Members of these genera are widely distributed in coastal habitats and frequently occur on hard substrates and sediments

in reef systems. The present observations therefore expand the morphological documentation of several representatives of these genera from Indonesian coral reef environments.

An important aspect of this study is the use of SEM to examine small benthic diatoms that possess relatively few diagnostic characters visible under light microscopy. Several of the taxa examined here, particularly *Psammodictyon* and small species of *Nitzschia*, exhibit subtle ultrastructural features that are difficult to resolve using LM alone. SEM observations therefore provide essential information on valve ornamentation, raphe structure, fibula arrangement, and striae organization, which are important characters for reliable taxonomic interpretation. Taken together, the combined LM and SEM observations presented here contribute additional morphological data for several small benthic diatoms associated with Indonesian coral reef habitats. Such detailed ultrastructural documentation remains important for improving the taxonomic understanding of inconspicuous benthic diatoms that are often underrepresented in broader floristic surveys.

4. CONCLUSIONS

This study documents five benthic diatom taxa isolated from coral reef habitats of Bawean Island, East Java, Indonesia, namely *Psammodictyon* sp., *Halamphora cf. oceanica*, *Halamphora yundangensis*, *Halamphora* sp., and *Nitzschia arauriae*. Observations using light microscopy (LM) and scanning electron microscopy (SEM) provided complementary morphological information, allowing reliable taxonomic characterization based on valve outline, striae density, raphe morphology, and other ultrastructural features. In particular, SEM observations revealed diagnostic characters that are difficult to resolve using LM alone, especially for small benthic diatoms with limited visible morphological features. The results provide additional morphological documentation of several benthic diatoms associated with Indonesian coral reef habitats and contribute to improving the taxonomic knowledge of inconspicuous marine diatom taxa from tropical environments.

AUTHOR INFORMATION

Corresponding Author

Oktiyas Muzaky Luthfi — Department of Marine Science, Universitas Brawijaya, Malang-65145 (Indonesia);

 orcid.org/0000-0002-9550-9381

Email: omuzakyl@ub.ac.id

Authors

Yenny Risjani — Center for Alga and Aquatic Environment /ALGAEN, Universitas Brawijaya, Malang-65145 (Indonesia);

 orcid.org/0000-0002-6191-5824

Rendha Agustina Ramawati — Department of Aquatic Resources Management, Universitas Brawijaya, Malang-65145 (Indonesia);

 orcid.org/0000-0001-8813-3649

Andrzej Witkowski — Institute of Marine and Environmental Sciences, University of Szczecin, Szczecin-70453 (Poland);

 orcid.org/0000-0002-1542-5373

Author Contributions

O. M. L.; Conceptualization, methodology, writing – original draft preparation, interpreted the original draft and conducted the methodology, and discussed the result. Y. R.; Writing – review & editing, supervision, project administration, and funding acquisition. R. A. R.; Formal analysis, investigation, and resources. A. W.; identification and interpretation of diatom taxa.

Conflicts of Interest

The authors declare no conflict of interest.

ACKNOWLEDGEMENT

This research was partially supported by the International Society for Diatom Research through the Luc Ector Early Career Award 2023.

DECLARATION OF GENERATIVE AI AND AI-ASSISTED TECHNOLOGIES IN THE MANUSCRIPT PREPARATION

Not applicable

REFERENCES

- [1] S. Blanco. (2020). In: "Modern Trends in Diatom Identification: Fundamentals and Applications". 25–38. [10.1007/978-3-030-39212-3_3](https://doi.org/10.1007/978-3-030-39212-3_3).
- [2] Y. Risjani, A. Witkowski, A. Kryk, Yuniata, E. Górecka, M. Krzywda, I. Safitri, A. Sapar, P. Dąbek, S. Arsad, E. Gusev, Rudiyansyah, Ł. Peszek, and R. J. Wróbel. (2021). "Indonesian Coral Reef Habitats Reveal Exceptionally High Species Richness and Biodiversity of Diatom Assemblages". *Estuarine, Coastal and Shelf Science*. **261** : 107551. [10.1016/j.ecss.2021.107551](https://doi.org/10.1016/j.ecss.2021.107551).
- [3] O. M. Luthfi, A. H. Priyambodo, M. Handayani, Y. Risjani, and A. Witkowski. (2023). "Epipsammic Diatom Cocconosis sp. as New Bioeroder in Scleractinian Coral". *Jurnal Ilmiah Perikanan dan Kelautan*. **15** (1). [10.20473/jipk.v15i1.37653](https://doi.org/10.20473/jipk.v15i1.37653).
- [4] A. Kryk, A. Witkowski, L. Ribeiro, J. P. Kociolek, S. Mayama, R. J. Wróbel, Y. Risjani, Yuniata, J. Bemiasa, and E. Bemanaja. (2021). "Novel Diatoms (Bacillariophyta) from Tropical and Temperate Marine Littoral Habitats with the Description of *Catenulopsis* gen. nov., and Two *Catenula* Species". *Diatom Research*. **36** (3): 265–280. [10.1080/0269249X.2021.1974572](https://doi.org/10.1080/0269249X.2021.1974572).
- [5] J. C. Taylor, W. R. Harding, and C. G. M. Archibald. "An Illustrated Guide to Some Common Diatom Species from South Africa". Water Research Commission, Pretoria.
- [6] Q. M. You, J. P. Kociolek, and Q. X. Wang. (2015). "Taxonomic Studies of the Diatom Genus *Halamphora* (Bacillariophyceae) from the Mountainous Regions of Southwest China, Including the Description of Two New Species". *Phytotaxa*. **205** (2): 75–89. [10.11646/phytotaxa.205.2.1](https://doi.org/10.11646/phytotaxa.205.2.1).
- [7] H. F. Olivares-Rubio, L. I. Cabrera, J. L. Godínez-Ortega, L. Salazar-Coria, and A. Vega-Lopez. (2017). "*Halamphora oceanica* (Catenulaceae, Bacillariophyta), a New Species from the Epipelagic Region of the Southwestern Gulf of Mexico". *Phytotaxa*. **317** (3): 188–198. [10.11646/phytotaxa.317.3.3](https://doi.org/10.11646/phytotaxa.317.3.3).
- [8] W. Wu, H. Lin, V. Patil, J. P. Kociolek, L. Sun, X. Li, J. Liang, C. Chen, and Y. Gao. (2020). "A New Marine Epiphytic Diatom Species, *Halamphora yundangensis* sp. nov. (Bacillariophyceae), from Yundang Lake, Southeast Coast of China". *Phytotaxa*. **450** (2). [10.11646/phytotaxa.450.2.6](https://doi.org/10.11646/phytotaxa.450.2.6).
- [9] R. M. Olszyński, E. Górecka, R. Trobajo, R. Gastineau, M. Ashworth, and D. G. Mann. (2025). "Taxonomic Review of *Tryblionella* with Special Reference to the Apiculatae Group: New Characters of Genus *Tryblionella* sensu stricto (Bacillariaceae)". *Journal of Phycology*. **61** (2): 330–352. [10.1111/jpy.70004](https://doi.org/10.1111/jpy.70004).
- [10] O. M. Luthfi, S. Arsad, A. Kryk, Y. Risjani, Yuniata, M. Rybak, Ł. Peszek, R. J. Wróbel, J. L. Pappas, M. Bąk, and A. Witkowski. (2024). "New Genera and New Species of Catenulaceae (Bacillariophyta) from Coral Reef Habitat of Two Indonesia Islands—Bawean and Sulawesi—A Morphological Approach". *PhytoKeys*. **248** : 263–291. [10.3897/phytokeys.248.131839](https://doi.org/10.3897/phytokeys.248.131839).
- [11] I. Renberg. (1990). "A Procedure for Preparing Large Sets of Diatom Slides from Sediment Cores". *Journal of Paleolimnology*. **4** (1): 87–90. [10.1007/BF00208301](https://doi.org/10.1007/BF00208301).
- [12] R. R. L. Guillard. (1975). "Culture of Marine Invertebrate Animals". Springer.
- [13] P. Boden. (1991). "Reproducibility in the Random Settling Method for Quantitative Diatom Analysis". *Micropaleontology*. 313–319. [10.2307/1485893](https://doi.org/10.2307/1485893).
- [14] R. W. Battarbee. (1986). "Proceedings of the Royal Irish Academy. Section B: Biological, Geological, and Chemical Science". *Proceedings of the Royal Irish Academy. Section B: Biological, Geological, and Chemical Science*.
- [15] A. Kryk, M. Bąk, E. Górecka, C. Riaux-Gobin, J. Bemiasa, E. Bemanaja, C. Li, P. Dąbek, and A. Witkowski. (2019). "Marine Diatom Assemblages of the Nosy Be Island Coasts, NW Madagascar: Species Composition and Biodiversity Using Molecular and Morphological Taxonomy".

- Systematics and Biodiversity*. **18** (2): 161–180. [10.1080/14772000.2019.1696420](https://doi.org/10.1080/14772000.2019.1696420).
- [16] K. Krammer and H. Lange-Bertalot. (1991). "Süßwasserflora von Mitteleuropa, Bd. 02/3: Bacillariophyceae: Teil 3: Centrales, Fragilariaceae, Eunotiaceae". Spektrum Akademischer Verlag.
- [17] A. Witkowski. (2000). "Diatom Flora of Marine Coasts I. Iconographia Diatomologica Annotated Diatom Micrographs. 925.
- [18] S. Sukandar, C. S. U. Dewi, and M. Handayani. (2017). "Analisis Kesesuaian dan Daya Dukung Lingkungan untuk Pengembangan Wisata Bahari di Pulau Bawean Kabupaten Gresik Provinsi Jawa Timur". *Depik: Jurnal Ilmu-Ilmu Perairan, Pesisir dan Perikanan*. **6** (3): 205–213. [10.13170/depik.6.3.7024](https://doi.org/10.13170/depik.6.3.7024).
- [19] C. S. U. Dewi and C. J. Harsindhi. (2018). "Karang dan Ikan Terumbu Pulau Bawean". Universitas Brawijaya Press.
- [20] L. Virta and P. Hedberg. (2024). "Declining Salinity and Increasing Temperature Reduce the Diversity and Resilience of Benthic Diatoms". *Environmental Microbiology*. **26** (2): e16569. [10.1111/1462-2920.16569](https://doi.org/10.1111/1462-2920.16569).
- [21] V. Berthon, A. Bouchez, and F. Rimet. (2011). "Using Diatom Life-Forms and Ecological Guilds to Assess Organic Pollution and Trophic Level in Rivers: A Case Study of Rivers in South-Eastern France". *Hydrobiologia*. **673** (1): 259–271. [10.1007/s10750-011-0786-1](https://doi.org/10.1007/s10750-011-0786-1).
- [22] A. Khoshmanesh, F. Lawson, and I. G. Prince. (1997). "Cell Surface Area as a Major Parameter in the Uptake of Cadmium by Unicellular Green Microalgae". *The Chemical Engineering Journal and The Biochemical Engineering Journal*. **65** (1): 13–19. [10.1016/S0923-0467\(96\)03091-6](https://doi.org/10.1016/S0923-0467(96)03091-6).
- [23] C. S. Lobban. (1983). "Colony and Frustule Morphology of Three Tube-Dwelling Diatoms from Eastern Canada". *Journal of Phycology*. **19** (3): 281–289. [10.1111/j.0022-3646.1983.00281.x](https://doi.org/10.1111/j.0022-3646.1983.00281.x).
- [24] T. Nakov, M. P. Ashworth, and E. C. Theriot. (2014). "Comparative Analysis of the Interaction Between Habitat and Growth Form in Diatoms". *The ISME Journal*. **9** (1): 246–255. [10.1038/ismej.2014.108](https://doi.org/10.1038/ismej.2014.108).
- [25] W. Zhu, Z. Ding, Y. Pan, and Q. Wang. (2022). "Using an Affinity Analysis to Identify Phytoplankton Associations". *Ecology and Evolution*. **12** (7). [10.1002/ece3.9047](https://doi.org/10.1002/ece3.9047).
- [26] L. Yang, Q. Yang, L. Lin, T. Luan, Q. Yang, P. Li, and N. F. Y. Tam. (2022). "Effects of Wetland, Tide, and Season on Benthic Biofilms and Related Sediment Properties in Mangrove Ecosystems". *Frontiers in Marine Science*. **9**. [10.3389/fmars.2022.1043826](https://doi.org/10.3389/fmars.2022.1043826).
- [27] S. R. Poltak and V. S. Cooper. (2010). "Ecological Succession in Long-Term Experimentally Evolved Biofilms Produces Synergistic Communities". *The ISME Journal*. **5** (3): 369–378. [10.1038/ismej.2010.136](https://doi.org/10.1038/ismej.2010.136).
- [28] Q. Yang, T. Liu, P. Yu, J. Zhang, J. P. Kociolek, Q. Wang, and Q. You. (2020). "A New Freshwater Psammodictyon Species in the Taihu Basin, Jiangsu Province, China". *Fottea*. **20** (2): 144–151. [10.5507/fot.2020.005](https://doi.org/10.5507/fot.2020.005).
- [29] S. N. P. Suriyanti and G. Usup. (2017). "Morphology and Molecular Phylogeny of the Marine Diatom *Nitzschia dentatum* sp. nov. and *N. johorensis* sp. nov. (Bacillariophyceae) from Malaysia". *Bangladesh Journal of Plant Taxonomy*. **24** (2): 183–196. [10.3329/bjpt.v24i2.35114](https://doi.org/10.3329/bjpt.v24i2.35114).
- [30] I. Louvrou and A. Economou-Amilli. (2012). "Transfer of Four Taxa of Genus *Nitzschia* Hassall to Genus *Psammodictyon* D.G. Mann (Bacillariophyceae)". *Journal of Biological Research*. **17** : 148.
- [31] B. J. Chohnoky. (1961). "Ein Beitrag zur Kenntnis der Diatomeenflora der Venetianischen Lagunen". *Hydrobiologia*. **17** (4): 287–325. [10.1007/BF00036337](https://doi.org/10.1007/BF00036337).
- [32] K. P. Cavalcante, P. I. Tremarin, E. G. Freire, and T. A. V. Ludwig. (2013). "Tryblionella persuadens comb. nov. (Bacillariaceae, Diatomeae): New Observations on Frustule Morphology of a Seldom Recorded Diatom". *Anais da Academia Brasileira de Ciências*. **85** (4): 1419–1426. [10.1590/0001-37652013108112](https://doi.org/10.1590/0001-37652013108112).

- [33] E. Kezlya, D. Kapustin, Z. Krivova, Y. Maltsev, L. Nguyen-Ngoc, D. T. N. Huynh, H. Doan-Nhu, and M. Kulikovskiy. (2025). "Comprehensive Analysis of the Diatom Genus *Psammodictyon* from Viet Nam: New Species, Molecular Data, and Fatty Acid Content". *Frontiers in Microbiology*. **16** : 1701605. [10.3389/fmicb.2025.1701605](https://doi.org/10.3389/fmicb.2025.1701605).
- [34] F. E. Round, R. M. Crawford, and D. G. Mann. (1990). "Diatoms: Biology and Morphology of the Genera". Cambridge University Press.
- [35] B. J. Cholnoky. (2018). "Die Diatomeenassoziationen der Santa-Lucia-Lagune in Natal (Südafrika)". De Gruyter. [10.1515/9783111388595](https://doi.org/10.1515/9783111388595).
- [36] H. F. Olivares-Rubio, L. I. Cabrera, J. L. Godínez-Ortega, L. Salazar-Coria, and A. Vega-López. (2017). "Halamphora oceanica (Catenulaceae, Bacillariophyta), a New Species from the Epipelagic Region of the Southwestern Gulf of Mexico". *Phytotaxa*. **317** (3): 188–198. [10.11646/phytotaxa.317.3.3](https://doi.org/10.11646/phytotaxa.317.3.3).
- [37] J. G. Stepanek and J. P. Kociolek. (2018). "Amphora and Halamphora from Coastal and Inland Waters of the United States and Japan".
- [38] J. G. Stepanek and J. P. Kociolek. (2015). "Three New Species of the Diatom Genus *Halamphora* (Bacillariophyta) from the Prairie Pothole Lakes Region of North Dakota, USA". *Phytotaxa*. **197** (1): 27–36. [10.11646/phytotaxa.197.1.3](https://doi.org/10.11646/phytotaxa.197.1.3).
- [39] J. G. Stepanek and J. P. Kociolek. (2019). "Molecular Phylogeny of the Diatom Genera *Amphora* and *Halamphora* (Bacillariophyta) with a Focus on Morphological and Ecological Evolution". *Journal of Phycology*. **55** (2): 442–456. [10.1111/jpy.12836](https://doi.org/10.1111/jpy.12836).
- [40] K. Krammer. (2000). "Diatoms of Europe: Diatoms of the European Inland Waters and Comparable Habitats. Volume 5: *Amphora sensu lato*". A.R.G. Gantner Verlag K.G.
- [41] D. V. Subba Rao and G. Wohlgeschaffen. (1990). "Morphological Variants of *Nitzschia pungens* Grunow f. *multiseries* Hasle". *Botanica Marina*. **33** (6): 545–554. [10.1515/botm.1990.33.6.545](https://doi.org/10.1515/botm.1990.33.6.545).
- [42] E. A. Morales and M. L. Vis. (2007). "Epilithic Diatoms (Bacillariophyceae) from Cloud Forest and Alpine Streams in Bolivia, South America". *Proceedings of the Academy of Natural Sciences of Philadelphia*. **156** (1): 123–155. [10.1635/0097-3157\(2007\)156\[123:EDBFCE\]2.0.CO;2](https://doi.org/10.1635/0097-3157(2007)156[123:EDBFCE]2.0.CO;2).
- [43] K. I. Shorenko, Y. A. Podunai, O. I. Davidovich, and M. S. Kulikovskiy. (2016). "Morphological Variation of Two Marine Diatom Species, *Nitzschia ventricosa* and *Ardissonea crystallina* (Bacillariophyta)". *Marine Biological Journal*. **1** (4): 53–62. [10.21072/mbj.2016.01.4.07](https://doi.org/10.21072/mbj.2016.01.4.07).
- [44] R. Trobajo, L. Rovira, L. Ector, C. E. Wetzel, M. Kelly, and D. G. Mann. (2013). "Morphology and Identity of Some Ecologically Important Small *Nitzschia* Species". *Diatom Research*. **28** (1): 37–59. [10.1080/0269249X.2012.734531](https://doi.org/10.1080/0269249X.2012.734531).
- [45] K. Krammer. (1988). "Bacillariophyceae 2 Teil; Bacillariaceae, Epithemiaceae, Surirellaceae Süßwasserflora von Mitteleuropa". 1–539.